Model Predictive Control for the Navigation of a Nonholonomic Vehicle with Field-of-View Constraints

Spyros Maniatopoulos, Dimitra Panagou and Kostas J. Kyriakopoulos

***Abstract*— This paper considers the problem of navigating a differentially driven nonholonomic vehicle while maintaining visibility with a (stationary) target by means of Model Predictive Control (MPC). The approach combines the convergence properties of a dipolar vector field within a constrained nonlinear MPC formulation, in which visibility and input saturation constraints are encoded via recentered barrier functions. A dipolar vector field offers by construction a global feedback motion plan to a goal configuration, yet it does not ensure that visibility is always maintained. For this reason, it is suitably combined with recentered barrier functions so that convergence to the goal and satisfaction of visibility and input constraints are both achieved. The control strategy falls into the class of dual-mode MPC schemes and its efficacy is demonstrated through simulation results in the case of a mobile robot with unicycle kinematics.**

I. Introduction

Control of underactuated mechanical systems which are subject to additional state constraints is encountered in various applications within the fields of robotics, ranging from the classical motion planning problem to formation and coverage control of multiple nonholonomic agents. State constraints typically arise due to various reasons, for instance due to the requirement of avoiding obstacles or due to limited sensing/communication. Within the field of mobile robotics in particular, the problem of controlling a (group of) nonholonomic robot(s) so that it (each) maintains visibility with a fixed or moving target has recently been of increasing interest. Both single-agent [1]–[4] and multi-agent problems have been addressed [5], [6]. In these contributions, the problem of maintaining visibility is addressed either by properly switching among state feedback controllers [1], [3], or by planning feasible paths within optimal control formulations [2], [4].

Nevertheless, the problem of designing state feedback controllers for systems subject to complex dynamics, state and input constraints remains inherently difficult and challenging. In part due to this reason, as well as stimulated by the recent technological advances which have resulted in powerful computational platforms, Model Predictive Control (MPC) [7]–[9] has become a very attractive tool for addressing motion planning problems in constrained environments. MPC-based solutions for robot navigation in obstacle environments have been presented, among others, in [10]–[15]. In the same spirit, the problem of navigating a nonholonomic vehicle while maintaining visibility with respect to (w.r.t.) to a target can be formulated as a constrained nonlinear MPC problem. To the best of our knowledge, there is not much work towards this direction. A very recent paper has appeared in [16], which considers the problem of obstacle avoidance along with visibility maintenance for an unmanned aerial vehicle; in this work the vehicle is forced to track a reference trajectory, while quadratic costs encode the misalignment of the vehicle's orientation w.r.t. the line-of-sight in order to handle visibility maintenance.

In this paper we consider the problem of navigating a nonholonomic mobile robot with field-of-view constraints while maintaining visibility w.r.t. a target of interest, and propose a solution based on MPC. The approach combines the notion of dipolar vector fields, developed in earlier work of ours [17], along with a nonlinear MPC formulation which handles both visibility and input constraints via recentered barrier functions [18]. The dipolar vector field serves as a global feedback motion plan to a goal configuration, yet the resulting trajectories may violate the visibility constraints. Thus, the MPC-based solution allows for both convergence to a desired configuration and satisfaction of the visibility and input constraints, since the control inputs are now generated based on both the misalignment of the robot w.r.t. the dipolar vector field and the constraints, over a prediction horizon.

The proposed algorithm falls into the class of dual-mode MPC schemes [7]. The system trajectories are forced by the model predictive controller into a suitably defined terminal region Ω which contains the goal configuration. Once in Ω, the system switches to the dipolar-based feedback controller, which ensures the convergence of the system trajectories to the goal configuration while not violating the visibility constraints; in other words, the terminal region Ω is a-priori determined such that the dipolar-based trajectories in Ω are both convergent and safe.

Compared to relevant works for the visibility maintenance problem which employ hybrid control solutions, see for instance [1], [3], the proposed approach offers a way of designing a control sequence that eliminates the need for switching, as well as the possible appearance of chattering when crossing the switching surfaces, and thus may be preferable from an application standpoint. Furthermore, the MPC formulation naturally allows for the straightforward incorporation of additional constraints which may encode, for

This work was supported by the EU funded project PANDORA: "Persistent Autonomy through learNing, aDaptation, Observation and ReplAnning", FP7–288273, 2012–2014.

Spyros Maniatopoulos is with the Sibley School of Mechanical and Aerospace Engineering, Cornell University, USA sm2296@cornell.edu

Dimitra Panagou is with the Coordinated Science Laboratory, College of Engineering, University of Illinois at Urbana-Champaign, USA dpanagou@illinois.edu

Kostas Kyriakopoulos is with the Control Systems Lab, School of Mechanical Engineering, National Technical University of Athens, Greece kkyria@mail.ntua.gr

instance, the requirement of keeping more than one objects in the camera field-of-view (f.o.v.), or other performance criteria. Finally, let us mention that, although the problem description is similar to [16], our approach differs in both the problem formulation, since here we use recentered barrier functions to encode the constraints into the running cost, and the objectives, since here we consider the misalignment w.r.t. the dipolar vector field, not the line-of-sight.

The paper is organized as follows: Section II presents the mathematical modeling for the considered problem, and Section III presents the formulation of the MPC strategy. The efficacy of the proposed control scheme is demonstrated in Section IV via simulation results. Our conclusions and thoughts on future extensions are summarized in Section V.

II. Mathematical Modeling

Let us consider the motion of a mobile robot with unicycle kinematics w.r.t. a global coordinate frame $\mathcal{G}$ described by:

$$\dot{\boldsymbol{q}} = \boldsymbol{G}(\boldsymbol{q})\boldsymbol{\nu} \Rightarrow \begin{bmatrix} \dot{x} \\ \dot{y} \\ \dot{\theta} \end{bmatrix} = \begin{bmatrix} \cos\theta & 0 \\ \sin\theta & 0 \\ 0 & 1 \end{bmatrix} \begin{bmatrix} u \\ \omega \end{bmatrix}, \tag{1}$$

where $\boldsymbol{q} = \begin{bmatrix} x & y & \theta \end{bmatrix}^\top \in Q$ is the configuration (state) vector comprising the position vector $\boldsymbol{r} = \begin{bmatrix} x & y \end{bmatrix}^\top$ and the orientation θ of the robot w.r.t. $\mathcal{G}$, $Q \subset \mathbb{R}^3$ is the configuration (state) space, $\boldsymbol{\nu} = \begin{bmatrix} u & \omega \end{bmatrix}^\top \in U$ is the vector of control inputs, $U \subset \mathbb{R}^2$ is a compact, convex set denoting the control space and u, ω are the linear and angular velocity of the robot, respectively, w.r.t. the body-fixed frame $\mathcal{B}$.

The motion of the robot is subject to state constraints due to limited sensing; the available sensor suite includes an onboard camera of limited angle-of-view a and two laser pointers. The target of interest and the laser dots projected on camera image plane are tracked via computer vision algorithms, and this information is processed online to provide the state (or pose) vector $\boldsymbol{q} \in Q$ of the robot w.r.t. the global frame $\mathcal{G}$, which lies on the center of the target (Fig. 1). For a detailed description of the sensor system the reader is referred to [19].

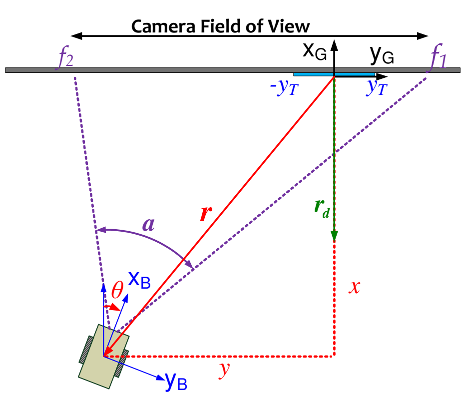

Fig. 1. Modeling of the state constraints imposed by the sensor system

Consequently, for the sensor system to be effective:

- the target should always be visible in the camera f.o.v., that reads: $[-y_T, y_T] \subseteq [f_2, f_1]$ (Fig. 1), where $2y_T > 0$ is the width of the target.
- the distance $\|\boldsymbol{r}\| = \sqrt{x^2+y^2}$ of the robot w.r.t. the target should not exceed a maximum range $R_{\max}$, so that the laser dots on the image plane can be detected by the computer vision algorithms.

These requirements impose a set of inequality constraints of the form $c_j(x, y, \theta) \geq 0$, which determine a subset $K \subset Q$ where the system trajectories $\boldsymbol{q}(t)$ should always evolve. The analytical expression of the constraints is given as:

$$c_1 : -y + x\tan(\theta - \frac{a}{2}) - y_T \geq 0, \tag{2a}$$

$$c_2 : -y_T + y - x\tan(\theta + \frac{a}{2}) \geq 0, \tag{2b}$$

$$c_3 : R_{\max}^2 - x^2 - y^2 \geq 0, \tag{2c}$$

and thus the admissible (safe) set K is defined as $K = \{\boldsymbol{q} \in Q \mid c_j(\boldsymbol{q}) \geq 0,\ j \in \{1,2,3\}\}$. Therefore, the task is to control the robot so that it converges to a goal state $\boldsymbol{q_d} = \begin{bmatrix} x_d & y_d & \theta_d \end{bmatrix}^\top \in K$, while the requirements on the sensor system being effective are always met.

A. State feedback control using dipolar vector fields

A state feedback control solution for the convergence of the unicycle to a goal state $\boldsymbol{q_d} \in \mathcal{Q}$ can be given using the concept of *dipolar* vector fields [17]. A dipolar vector field $\mathbf{F} : \mathbb{R}^2 \to \mathbb{R}^2$ is by construction non-vanishing everywhere on $\mathbb{R}^2$ except for the origin $(0, 0)$, which is the unique critical point of dipole type [20]; this implies that all integral curves begin and end at the origin $(x, y) = (0, 0)$ of the global frame $\mathcal{G}$. The analytical form of $\mathbf{F} : \mathbb{R}^2 \to \mathbb{R}^2$ is:

$$\mathbf{F}(\boldsymbol{r}) = \lambda(\boldsymbol{p}^\top \boldsymbol{r})\boldsymbol{r} - \boldsymbol{p}(\boldsymbol{r}^\top \boldsymbol{r}), \tag{3}$$

where $\lambda \geq 2$, $\boldsymbol{p} \in \mathbb{R}^2$ and $\boldsymbol{r}$ is the position vector w.r.t. $\mathcal{G}$. The main characteristic of the vector field (3) is that the integral curves are symmetric w.r.t. the axis of the vector $\boldsymbol{p}$. Then, choosing the vector $\boldsymbol{p} = \begin{bmatrix} p_x & p_y \end{bmatrix}^\top$ such that $\varphi_p = \operatorname{atan2}(p_y, p_x) \triangleq \theta_d$, reduces the orientation control of the unicycle into forcing it to align with the integral curves of the dipolar vector field (3). Furthermore, if the vector $\boldsymbol{p}$ is assigned on a desired position $\boldsymbol{r_d} = \begin{bmatrix} x_d & y_d \end{bmatrix}^\top$, then one gets a dipolar vector field whose integral lines converge to $\boldsymbol{r_d}$ with the desired orientation $\varphi_p \triangleq \theta_d$.

Thus, for $\lambda = 3$ and $\boldsymbol{p} = \begin{bmatrix} 1 & 0 \end{bmatrix}^\top$ we define the 2-dimensional vector field $\mathbf{F}(\cdot) = \mathrm{F}_x \frac{\partial}{\partial x} + \mathrm{F}_y \frac{\partial}{\partial y}$:

$$\mathrm{F}_x = 2(x - x_d)^2 - (y - y_d)^2, \tag{4a}$$

$$\mathrm{F}_y = 3(x - x_d)(y - y_d), \tag{4b}$$

which is non-singular everywhere in $\mathbb{R}^2$ except for the desired position $\boldsymbol{r} = \boldsymbol{r_d}$, and its integral curves converge to $\boldsymbol{r_d}$ with direction $\phi \triangleq \operatorname{atan2}(\mathrm{F}_y, \mathrm{F}_x) \to \varphi_p \triangleq \operatorname{atan2}(1, 0) = 0$, i.e. parallel to the x_G axis.

Thus, the control for the unicycle reduces to designing a feedback control law so that the unicycle aligns with the dipolar vector field (4), and follows the integral curves until converging to (x_d, y_d). This can be achieved via a state feedback control law $\boldsymbol{\gamma}(\boldsymbol{q}) : \mathbb{R}^3 \to \mathbb{R}^2$, given as:

$$u = -k_1 \operatorname{sgn}\left((\boldsymbol{r} - \boldsymbol{r_d})^\top \left[\begin{smallmatrix}\cos\theta \\ \sin\theta\end{smallmatrix}\right]\right) \tanh(||\boldsymbol{r} - \boldsymbol{r_d}||^2), \quad (5a)$$

$$\omega = -k_2(\theta - \phi) + \dot{\phi}, \quad (5b)$$

where $k_1,\ k_2 > 0$, and $\phi = \operatorname{atan2}(\mathrm{F}_y, \mathrm{F}_x)$ is the reference direction of the vector field at (x, y) (cf. [17]).

However, controlling the robot so that it tracks the vector field (4) may result in trajectories $\boldsymbol{q}(t)$ which may force the robot to lose visibility w.r.t. the target for some finite time interval, i.e. may violate at least one of the visibility constraints (2). In earlier work of ours [21] we addressed a similar problem for an underactuated marine vehicle by means of state-dependent switching control. Nevertheless, using such a control strategy may suffer from the appearance of chattering across the switching surface(s) during some finite time, which in general is undesirable for this class of mechanical systems. To overcome this limitation, in this paper we propose a control solution that is based on MPC, or receding horizon control [7].

III. Predictive Control Design

MPC relies on iterative, finite horizon optimization. At each calculation time t, the current state $\boldsymbol{q}(t)$ is measured or estimated, and a control law that optimizes a suitably selected cost functional over a time interval $[t, t+T_p)$ is computed, where T_p is the prediction horizon. The obtained control law is applied over a shorter finite horizon $0 < T_c < T_p$ (control horizon), and the process is repeated at the new state $\boldsymbol{q}(t+T_c)$.

A. The Finite Horizon Optimal Control Problem

For the problem considered here, the open-loop, Finite Horizon Optimal Control Problem (FHOCP) at time t with initial state $\boldsymbol{q}(t)$ is formulated as:
Find:

$$\min_{\bar{\boldsymbol{\nu}}(\tau)} J(\boldsymbol{q}(t), \bar{\boldsymbol{\nu}}(\cdot); T_p) \quad (6)$$

where:

$$J(\boldsymbol{q}(t), \bar{\boldsymbol{\nu}}(\cdot); T_p) = \int_t^{t+T_p} \left(L\left(\bar{\boldsymbol{q}}(\tau), \bar{\boldsymbol{\nu}}(\tau)\right)\right) d\tau + \\ + M\left(\bar{\boldsymbol{q}}(t+T_p)\right) \quad (7)$$

subject to:

$$\dot{\bar{\boldsymbol{q}}}(\tau) = \boldsymbol{G}(\bar{\boldsymbol{q}}(\tau))\bar{\boldsymbol{\nu}}(\tau), \quad \bar{\boldsymbol{q}}(t; \boldsymbol{q}(t), t) = \boldsymbol{q}(t) \quad (8a)$$

$$\bar{\boldsymbol{\nu}}(\tau) \in U, \quad \bar{\boldsymbol{q}}(\tau) \in K, \quad \tau \in [t, t+T_p] \quad (8b)$$

$$\bar{\boldsymbol{q}}\left(t+T_p; \boldsymbol{q}(t), t\right) \in \Omega, \quad (8c)$$

where $L(\boldsymbol{q}, \boldsymbol{\nu})$ is a positive definite function denoting the incremental (or running) cost, $M(\boldsymbol{q})$ is a positive definite function denoting the terminal cost (or cost-to-go), T_p is the (fixed) finite prediction horizon and $\bar{\boldsymbol{q}}(\ \cdot\ ; \boldsymbol{q}(t), t)$ is the trajectory of (8a), starting at $\boldsymbol{q}(t)$ at time t and driven by $\bar{\boldsymbol{\nu}} : [t, t+T_p] \to U$. Note that we have used the notation $(\bar{\boldsymbol{q}}, \bar{\boldsymbol{\nu}})$ as in [8], to denote the internal variables in the model predictive controller, i.e. the predicted states $\bar{\boldsymbol{q}}$ within the controller $\bar{\boldsymbol{\nu}}$, which need not and will not be the same as the actual states $\boldsymbol{q}(t)$ of the real system.

The terminal inequality constraint (8c) forces the states at the end of the finite prediction horizon to be in some set Ω containing the goal state $\boldsymbol{q_d}$, called the terminal region [8]. For the problem considered here, the terminal region Ω is chosen as:

$$\Omega = \left\{ \boldsymbol{q} \in K \;\middle|\; \begin{matrix} \|\boldsymbol{r} - \boldsymbol{r_d}\| \leq r_0, |\theta - \phi(x,y)| \leq \varepsilon_1 \\ |\pi - \operatorname{atan2}(y - y_d, x - x_d)| \leq \varepsilon_2, \end{matrix} \right\},$$

where $r_0, \varepsilon_1, \varepsilon_2$ are positive parameters determined off-line, so that Ω is a subset of the safe set K containing the goal state $\boldsymbol{q_d}$. For the states $\boldsymbol{q} \in \Omega$ the dipolar-based feedback controller (5) guarantees the convergence of the system trajectories $\boldsymbol{q}(t)$ to the goal state $\boldsymbol{q_d}$ without violating the visibility constraints (2). In other words, the closed-loop trajectories $\boldsymbol{q}(t) \in \Omega$ under (5) are both safe and convergent to $\boldsymbol{q_d}$. Thus, when the system trajectories reach the terminal region Ω, the system switches to the dipolar-based controller; in this sense, the proposed state feedback control strategy falls into the class of dual-mode MPC schemes.

B. Running and Terminal Costs

The objective functional (7) consists of a running cost $L\left(\bar{\boldsymbol{q}}(\tau), \bar{\boldsymbol{\nu}}(\tau)\right)$, where $\tau \in [t, t+T_p]$, to specify the desired control performance, and the terminal cost $M(\bar{\boldsymbol{q}}(t+T_p))$, to specify the states at the end of the prediction horizon. The running $L(\cdot,\cdot)$ and terminal $M(\cdot)$ costs are defined as:

$$L(\boldsymbol{q}, \boldsymbol{\nu}) = \frac{1}{2}\left(\boldsymbol{z}^\top \boldsymbol{Q} \boldsymbol{z} + \boldsymbol{\nu}^\top \boldsymbol{R} \boldsymbol{\nu}\right) + B_{\boldsymbol{q}}(\boldsymbol{q}, \boldsymbol{q_d}) + B_{\boldsymbol{\nu}}(\boldsymbol{\nu}), \quad (9a)$$

$$M(\boldsymbol{q}) = \frac{1}{2}\boldsymbol{z}^\top \boldsymbol{P} \boldsymbol{z}, \quad (9b)$$

where $\boldsymbol{z} = \begin{bmatrix} x - x_d & y - y_d & \theta - \phi(x,y) \end{bmatrix}^\top$, $\phi(x,y)$ is the orientation of the vector field $\mathbf{F}(\cdot,\cdot)$ at a point (x,y), $\boldsymbol{Q}, \boldsymbol{P} \in \mathbb{R}^{3\times3}$ and $\boldsymbol{R} \in \mathbb{R}^{2\times2}$ are positive definite weighting matrices, and $B_{\boldsymbol{q}}(\boldsymbol{q}, \boldsymbol{q_d})$, $B_{\boldsymbol{\nu}}(\boldsymbol{\nu})$ are suitably defined *recentered barrier functions* [18], which are used to account for the visibility (state) and input constraints, respectively.[1] The terminal cost $M(\cdot)$ is a quadratic function of the position error $e = \|\boldsymbol{r} - \boldsymbol{r_d}\|$ and the orientation error $s = \theta - \phi(x,y)$ of the robot w.r.t. the vector field $\mathbf{F}$, and can be used as a Lyapunov-like function to establish convergence of system trajectories $\boldsymbol{q}(t)$ to $\boldsymbol{q_d}$ using the invariance principle [17].

C. Constraint embedding via recentered barrier functions

The concept of *recentered* barrier functions [18] has been introduced in order to not only regulate the solution to lie in the interior of the constrained set, but also to ensure that, if the system converges, then it converges to a desired point.

[1]Note that, contrary to other relevant work that penalize the deviation from a reference trajectory $\boldsymbol{q_r}(t)$, in our formulation we penalize the "misalignment" of the robot orientation θ w.r.t. the reference direction $\phi(x,y)$ of the vector field $\mathbf{F}(\cdot,\cdot)$ at (x,y), as well as the distance of the robot w.r.t. (x_d, y_d)

For ensuring that the visibility constraints (2) are never violated, we first define a barrier function $b_j(\cdot) : \mathbb{R}^3 \to \mathbb{R}^+$ for each one of the constraints (2), as $b_j(\cdot) = \frac{1}{c_j(\cdot)}$, which tends to $+\infty$ as $c_j(\cdot) \to 0$, $j \in \{1, 2, 3\}$. Then, the gradient recentered barrier function [18] for each constraint $c_j(\cdot)$ is given as:

$$r_j(\boldsymbol{q}) = b_j(\boldsymbol{q}) - b_j(\boldsymbol{q_d}) - \nabla b_j(\boldsymbol{q_d})^\top (\boldsymbol{q} - \boldsymbol{q_d}),$$

and is positive everywhere, except for $\boldsymbol{q_d}$; this property ensures that the cost functional $L(\cdot, \cdot)$ is positive everywhere except for $(\boldsymbol{q}, \boldsymbol{\nu}) = (\boldsymbol{q_d}, \mathbf{0})$. The recentered barrier function $B_{\boldsymbol{q}}(\boldsymbol{q}, \boldsymbol{q_d})$ which takes into account all visibility (state) constraints is defined as:

$$B_{\boldsymbol{q}}(\boldsymbol{q}, \boldsymbol{q_d}) = \sum_{j=1}^{3} r_j(\boldsymbol{q}).$$

The function $B_{\boldsymbol{q}}(\boldsymbol{q}, \boldsymbol{q_d})$ tends to $+\infty$ as $c_j(\boldsymbol{q}) \to 0$ and vanishes at $\boldsymbol{q_d}$ only.

Likewise, for ensuring that the saturation constraints on the controls u, ω are never violated, i.e. that $-u_{\max} \leq u \leq u_{\max}$ and $-\omega_{\max} \leq \omega \leq \omega_{\max}$, where $u_{\max}$, $\omega_{\max} > 0$, we define the recentered barrier function $B_{\boldsymbol{\nu}}(\boldsymbol{\nu})$ as:

$$\begin{aligned} B_{\boldsymbol{\nu}}(\boldsymbol{\nu}) = &-\frac{2}{u_{\max}} + \frac{1}{-u + u_{\max}} + \frac{1}{u + u_{\max}} - \\ &- \frac{2}{\omega_{\max}} + \frac{1}{-\omega + \omega_{\max}} + \frac{1}{\omega + \omega_{\max}}, \end{aligned}$$

which vanishes only at $\boldsymbol{\nu} = \mathbf{0}$ and goes to $+\infty$ at the boundary of $U = [-u_{\max}, u_{\max}] \times [-\omega_{\max}, \omega_{\max}]$.

D. Convergence under the MPC *scheme*

Convergence of our MPC-based algorithm is directly derived via the sufficient conditions in [7]. First, note that the system (1) satisfies the following assumptions, taken from [8, Theorem 1] and presented in the original notation:
For the class of nonlinear systems described by:

$$\dot{\mathbf{x}} = \mathbf{f}(\mathbf{x}, \mathbf{u}), \quad \mathbf{x}(0) = \mathbf{x_0},$$

where $\mathbf{u}(t) \in \mathcal{U}$, $\forall t \geq 0$, $\mathbf{x}(t) \in \mathcal{X}$, $\forall t \geq 0$, assume that:

- (A_1) $\mathcal{U} \subset \mathbb{R}^p$ is compact, $\mathcal{X} \subseteq \mathbb{R}^n$ is connected and $(0, 0) \in \mathcal{X} \times \mathcal{U}$.
- (A_2) The vector field $\mathbf{f} : \mathbb{R}^n \times \mathbb{R}^m \to \mathbb{R}^n$ is continuous and satisfies $\mathbf{f}(\mathbf{0}, \mathbf{0}) = \mathbf{0}$. In addition, it is locally Lipschitz continuous in $\mathbf{x}$.
- (A_3) The system has a unique continuous solution for any initial condition in the region of interest and any piecewise continuous and right continuous input function $\mathbf{u}(\cdot) : [0, T_p] \to \mathcal{U}$.
- (A_4) the running cost $L : \mathbb{R}^n \times \mathcal{U} \to \mathbb{R}$ is continuous in all arguments with $L(\mathbf{0}, \mathbf{0}) = 0$ and $L(\mathbf{x}, \mathbf{u}) \geq 0$, $\forall (\mathbf{x}, \mathbf{u}) \in \mathbb{R}^n \times \mathcal{U} \setminus \{\mathbf{0}, \mathbf{0}\}$.
- (A_5) The nonlinear FHOCP has a feasible solution for $t = 0$.

Clearly, assumptions $(A_1$–$A_3)$ are satisfied for the system (1), with $\mathbf{x} = \mathbf{0}$ corresponding to the desired configuration $\boldsymbol{q} = \boldsymbol{q_d}$. The construction of the running cost (9a) satisfies assumption (A_4), as explained in the previous subsection. Finally, assumption (A_5) depends on the prediction horizon T_p. Therefore, T_p cannot be freely chosen; it is a tuning parameter that should be chosen large enough as to guarantee that the FHOCP (6)–(8) is feasible at $t = 0$.

The remaining ingredients (terminal cost, terminal region, local controller) that are required to establish convergence guarantees, should satisfy the sufficient conditions in [7]:

- (B_1) $\Omega \subset K$, Ω closed, $\boldsymbol{q}_d \in \Omega$,
- (B_2) $\boldsymbol{\gamma}(\boldsymbol{q}) \in U$, $\forall \boldsymbol{q} \in \Omega$,
- (B_3) Ω is positively invariant under $\dot{\boldsymbol{q}} = \boldsymbol{G}(\boldsymbol{q})\boldsymbol{\gamma}(\boldsymbol{q})$,
- (B_4) $M(\cdot)$ is a local control Lyapunov function.

Condition (B_1) for Ω is satisfied by construction. Satisfaction of condition (B_2) is achieved by tuning the gains k_1, k_2 of the local, dipolar vector field based control law $\boldsymbol{\gamma}(\boldsymbol{q})$, given by (5). The terminal cost $M(\cdot)$ is a quadratic function of the position error $e = \|\boldsymbol{r} - \boldsymbol{r_d}\|$ and the orientation error $s = \theta - \phi(x, y)$ of the robot w.r.t. the vector field $\mathbf{F}(\cdot)$, and can be used as a Lyapunov-like function to establish convergence of system trajectories $\boldsymbol{q}(t) \in \Omega$ to $\boldsymbol{q_d}$, as shown in [17]; thus condition (B_4) is also satisfied. Finally, satisfaction of condition (B_3) trivially follows from the construction of Ω and the control law (5), since the system is forced to align with and flow along a safe integral curve of $\mathbf{F}$.

IV. Simulation Results

The performance of the resulting system trajectories is evaluated through various simulation scenarios. To highlight the effectiveness of the MPC strategy over using the dipolar vector field based control law only, both controllers have been simulated for the same initial and final conditions.

The robot initiates at $\boldsymbol{q}(0) = \begin{bmatrix} -8 & -10 & \frac{\pi}{4} \end{bmatrix}^\top$ while the goal state is set as $\boldsymbol{q_d} = \begin{bmatrix} -1 & 0 & 0 \end{bmatrix}^\top$. The angle-of-view is set to $a = 60$ deg, $y_T = 0.2$ m, and $R_{\max} = 13$ m. For the MPC simulations, the sampling time has been set to $\delta = 1$, the prediction horizon to $T_p = 30$ time steps, and the control horizon to $T_c = 5$ time steps.

Fig. 2(a) illustrates the path followed under (5), which forces the robot to align with the dipolar vector field $\mathbf{F}$ while moving towards the goal position; clearly, the visibility constraints are violated. Fig. 2(b) illustrates the path obtained from the MPC scheme, for the robot starting at the same initial condition. As expected, the robot avoids to track the integral curves of the vector field $\mathbf{F}$ that would result in losing visibility with the target (note the resulting path for $-10 < y < -4$), while it aligns with them as it gets closer to the goal position, where the integral curves are by construction such that visibility with the target is maintained, see also Fig. 3. Under the MPC strategy, the robot converges into the terminal region Ω. Once in Ω, the system switches to the dipolar-based control law (5) (which by design renders the region Ω a positively invariant set), and the robot converges to $\boldsymbol{q_d}$. Note that the switch between the MPC inputs and the dipolar-based inputs is designed to be continuous, i.e. no jumps occur in the linear and the angular velocities at the time instant of switching, as also indicated

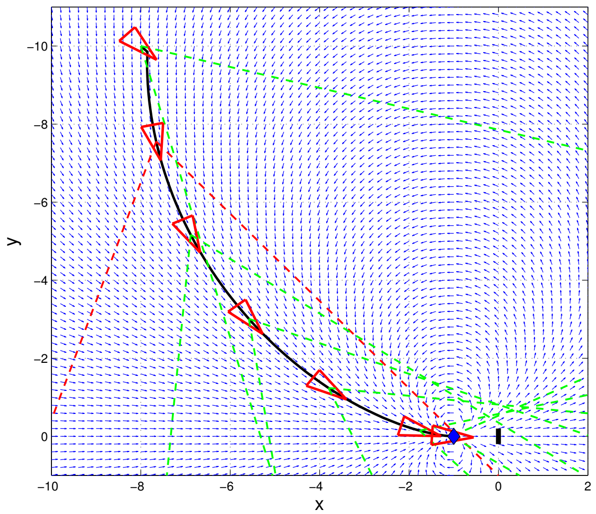

(a) The robot is controlled to track the dipolar vector field (4) on its way to $\boldsymbol{q_d}$, but loses visibility w.r.t. the target for some finite time interval.

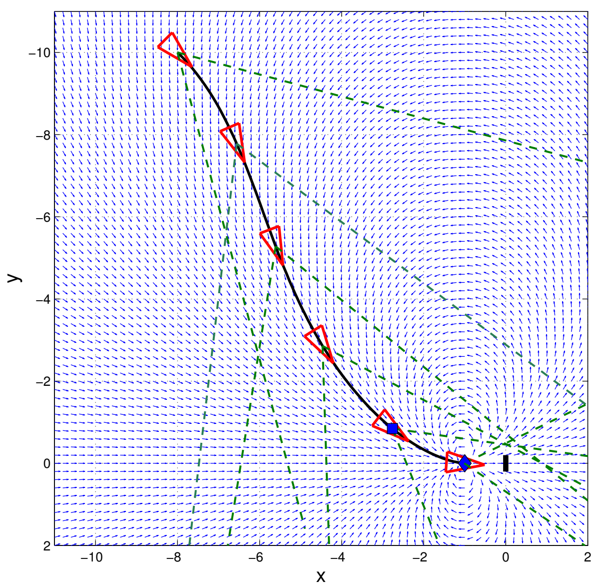

(b) The robot is controlled under the proposed MPC scheme, and converges to the terminal region Ω, while respecting the visibility constraints. Once in Ω, the system switches to the dipolar-based controller and the robot converges to $\boldsymbol{q_d}$.

Fig. 2. Comparison of the paths resulting from (5) and the MPC scheme.

in Fig. 4. The point in $\mathbb{R}^2$ where the system switches is indicated by the blue square in Fig. 2(b). The resulting control inputs $u(t), \omega(t)$ are shown in Fig. 4. Fig. 5 illustrates the paths followed by the robot for various initial conditions, while Fig. 6 shows the evolution of the constraint functions $c_j(\cdot)$, $j \in \{1, 2\}$, for each one of the cases considered.

V. Conclusions

This paper presented an MPC-based solution to the problem of navigating a nonholonomic mobile robot while maintaining visibility w.r.t. a target. The proposed approach combines the convergence properties of a dipolar vector field, along with a constrained nonlinear MPC formulation using recentered barrier functions, which take into account the visibility constraints and the saturation of control inputs. The control strategy falls into the class of dual-mode MPC schemes, i.e. the system trajectories are forced by the model predictive controller into a suitably defined terminal region containing the goal configuration; in this region, the trajectories resulting by tracking the dipolar vector field by construction do not violate the visibility constraints. The efficacy of the proposed approach was demonstrated through simulation results.

Future work can be towards the consideration of systems subject to dynamic (i.e. second order) nonholonomic constraints, such as underactuated marine vehicles, as well as towards the treatment of external disturbances and moving targets within the MPC framework.

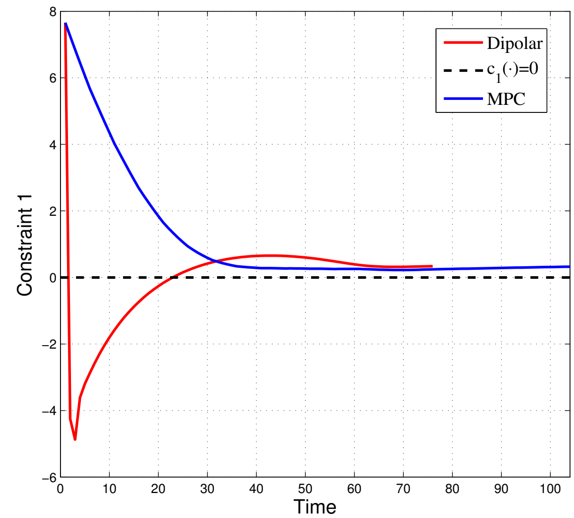

Fig. 3. The value of the constraint function $c_1(\cdot)$ is positive under the MPC scheme, implying that visibility is always maintained. In this scenario, the constraints $c_2(\cdot)$, $c_3(\cdot)$ are trivially satisfied and thus not depicted.

References

[1] G. Kantor and A. A. Rizzi, "Feedback control of underactuated systems via sequential composition: Visually guided control of a unicycle," in *Robotics Research*, P. Dario and R. Chatila, Eds. Springer Berlin Heidelberg, 2005, pp. 281–290.

[2] S. Bhattacharya, R. Murrieta-Cid, and S. Hutchinson, "Optimal paths for landmark-based navigation by differential-drive vehicles with field-of-view constraints," *IEEE Transactions on Robotics*, vol. 23, no. 1, pp. 47–59, Feb. 2007.

[3] G. A. D. Lopes and D. E. Koditschek, "Visual servoing for nonholonomically constrained three degree of freedom kinematic systems," *The International Journal of Robotics Research*, vol. 26, no. 7, p. 715736, July 2007.

[4] P. Salaris, D. Fontanelli, L. Pallotino, and A. Bicchi, "Shortest paths for a robot with nonholonomic and field-of view constraints," *IEEE Transactions on Robotics*, vol. 26, no. 2, pp. 269–280, Apr. 2010.

[5] N. Cowan, O. Shakernia, R. Vidal, and S. Sastry, "Vision-based follow-the-leader," in *Proc. of the 2003 IEEE/RSJ Intl. Conference on Intelligent Robots and Systems*, Las Vegas, Nevada, Oct. 2003, pp. 1796–1801.

[6] F. Morbidi, F. Bullo, and D. Prattichizzo, "Visibility maintenance via controlled invariance for leader-follower vehicle formations," *Automatica*, vol. 47, no. 5, pp. 1060–1067, May 2011.

[7] D. Mayne, J. Rawlings, C. Rao, and P. Scokaert, "Constrained model predictive control: Stability and optimality," *Automatica*, vol. 36, no. 6, pp. 789 – 814, 2000.

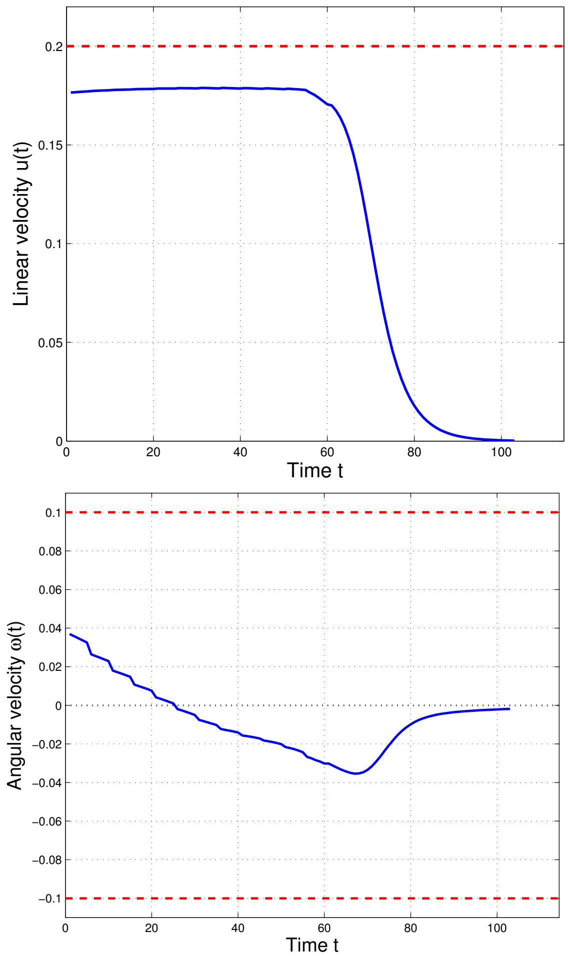

Fig. 4. The resulting control inputs $u(t)$, $\omega(t)$, respectively. Note that the saturation constraints $|u(t)| \leq u_{\max}$ and $|\omega(t)| \leq \omega_{\max}$ are always met.

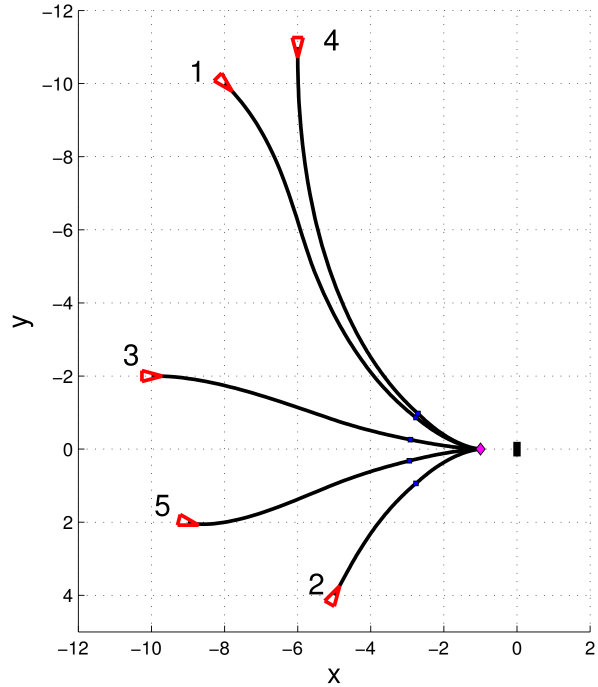

Fig. 5. Paths followed by the robot under the MPC scheme.

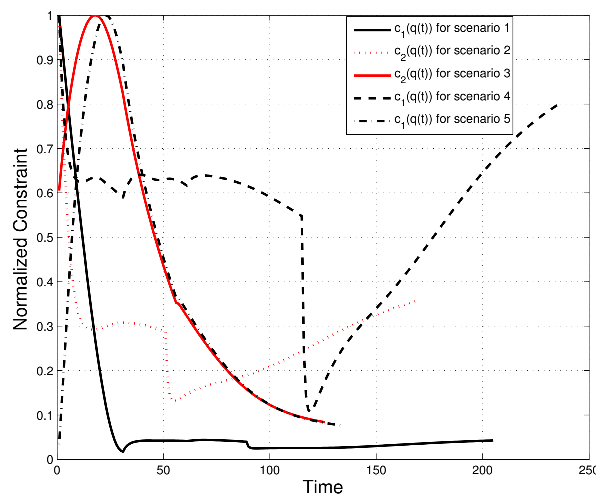

Fig. 6. Evolution of the constraint functions $c_j(\cdot)$ for the scenarios in Fig. 5. For each scenario, the constraint $c_j(\cdot)$ that gets closer to zero is depicted.

[8] H. Chen and F. Allgower, “A quasi-infinite horizon nonlinear model predictive control scheme with guaranteed stability,” *Automatica*, vol. 34, no. 10, pp. 1205–1217, 1998.

[9] R. Findeisen and F. Allgöwer, “An introduction to nonlinear model predictive,” in *Control, 21st Benelux Meeting on Systems and Control, Veidhoven*, 2002, pp. 1–23.

[10] P. Ögren and N. E. Leonard, “A convergent dynamic window approach to obstacle avoidance,” *IEEE Transactions on Robotics*, vol. 21, no. 2, pp. 188–195, Apr. 2005.

[11] J. L. Piovesan and H. G. Tanner, “Randomized model predictive control for robot navigation,” in *Proc. of the 2009 IEEE International Conference on Robotics and Automation*, Kobe, Japan, May 2009, pp. 94–99.

[12] A. Brooks, T. Kaupp, and A. Makarenko, “Randomised mpc-based motion-planning for mobile robot obstacle avoidance,” in *Proc. of the 2009 IEEE International Conference on Robotics and Automation*, Kobe, Japan, May 2009, pp. 3962–3967.

[13] Y. Yoon, J. Shin, H. J. Kim, Y. Park, and S. Sastry, “Model-predictive active steering and obstacle avoidance for autonomous ground vehicles,” *Control Engineering Practice*, vol. 17, p. 741750, 2009.

[14] T. Faulwasser, B. Kern, and R. Findeisen, “Model predictive path-following for constrained nonlinear systems,” in *Proc. of the 48th IEEE Conference on Decision and Control*, Shanghai, P.R. China, Dec. 2009, pp. 8642–8647.

[15] A. Tahirovic and G. Magnani, “Passivity-based model predictive control for mobile robot navigation planning in rough terrains,” in *Proc. of the 2010 IEEE/RSJ International Conference on Intelligent Robots and Systems*, Taipei, Taiwan, Oct. 2010, pp. 307–312.

[16] D. Lee, H. Lim, and H. J. Kim, “Obstacle avoidance using image-based visual servoing integrated with nonlinear model predictive control,” in *Proc. of the 50th IEEE Conference on Decision and Control and European Control Conference*, Orlando, Florida, Dec. 2011, pp. 5689–5694.

[17] D. Panagou, H. G. Tanner, and K. J. Kyriakopoulos, “Control of nonholonomic systems using reference vector fields,” in *Proc. of the 50th IEEE Conference on Decision and Control and European Control Conference*, Orlando, Florida, Dec. 2011, pp. 2831–2836.

[18] A. G. Wills and W. P. Heath, “A recentred barrier for constrained receding horizon control,” in *Proc. of the American Control Conference*, Anchorage, AK, USA, May 2002, pp. 4177–4182.

[19] G. C. Karras, S. G. Loizou, and K. J. Kyriakopoulos, “Towards semi-autonomous operation of under-actuated underwater vehicles: sensor fusion, on-line identification and visual servo control,” *Autonomous Robots*, vol. 31, pp. 67–86, July 2011.

[20] M. Henle, *A Combinatorial Introduction to Topology*. Dover Publications, 1994.

[21] D. Panagou and K. J. Kyriakopoulos, “Control of underactuated systems with viability constraints,” in *Proc. of the 50th IEEE Conference on Decision and Control and European Control Conference*, Orlando, Florida, Dec. 2011, pp. 5497–5502.